Sensors & Transducers, Vol. 21, Special Issue, May 2013, pp. 199-204

Sensors & Transducers

http://www.sensorsportal.com

Numerical Simulation of Gas-Solid Two-Phase Flow for Four-Channels Pulverized Swirling Burner

[1] Defu LI, Maozhao XIE, Chunyan SHEN, [*] Hongchao YIN, Hong LIU
[1, 2] Energy and Power Engineering, Dalian University of Technology, Liaoning, 116024, China
[*] E-mail: hcyin@dlut.edu.cn

Received: 9 April 2013 /Accepted: 14 May 2013 /Published: 30 May 2013

Abstract: This article presents a mathematical model of cold gas-solid two-phase flow which is based on the cement rotary kiln in service. By altering the parameters of air supply system of four- channels pulverized burner, investigations are taken of that motion trajectory and particle distributions in the very turbulent field. The results show that motion trail of most particles in rotary kiln is a combination process of gradual diffusion and slow sedimentation; increasing internal flow velocity would aggravate coal particles to diffuse; external flow velocity should be controlled in a reasonable range. *Copyright © 2013 IFSA.*

Keywords: Two-phase flow, Four- channels pulverized burner, Particle-trajectory model.

1. Introduction

Burner is a key component of combustion systems, by which air flow and fuel are blown to rotary kiln and form a specific flow structure that will contribute to rapid ignition and stable combustion. Hence, to achieve an excellent performance, the design and operation of burner is conclusive to economical efficiency and reliability for rotary kiln [1].

A good burner ensure rotary kiln operating in the most suitable thermotechnical condition for the cement production, which will obtain high grade, high efficient, low cost and long-term production, also meet the environmental requirement [2]. Therefore, the study on burner character is critical to cement industry development [3-6]. This article applies CFD to simulate 3-D four-channels pulverized burner by creating a cold model to simulate flow motion driven by multi-tunnel burner and particle distributions influenced by turbulent field. This is an attempt to provide theoretical basis to hot model combustion research.

2. Two-phase Flow Model Description

It is well known that the numerical model for simulating two-phase flow model can be described in two major methods [7-10]. One is two- fluid model, also named as EULERIAN-EULERIAN model in which particle is regarded as fluid. Particle and gas together are considered as in a coexisting and interpenetrating continuum model. The other is dispersed phase model, also called as EULERIAN-LAGRANGIAN model in which particle is considered discrete and gas is considered as continuum model. The interaction between each particle and ambient gas is calculated as well. In the paper, numerical investigation of particle motion trail is simulated by applying dispersed phase model, and two phases are coupled by interactive force, where particle phase is calculated in LAGRANGIAN coordinate, while continuous gas phase is calculated in EULERIAN coordinate.

Regardless of the pulsation from gas density and phase transition, and resistance, gas phase conservation equation can be written in a general form as [11]:

$$\frac{\partial}{\partial t}(\rho\phi) + \frac{\partial}{\partial x_j}(\rho v_j \phi) = \frac{\partial}{\partial x_j}(\Gamma_\phi \frac{\partial \phi}{\partial x_j}) + S_\phi + S_{\rho\phi} \quad (1)$$

where S_ϕ is the origin of gas phase; $S_{\rho\phi}$ is the origin of the interaction between gas phase and particle phase; ϕ, Γ_ϕ, S_ϕ and $S_{\rho\phi}$ are the usual source term, which are listed in [12].

3. Physical Model and Numerical Method

3.1. Physical Model

According to the reference [13], numerical investigations on coal particle was burned in cement rotary kiln, four-channel swirling burner was numerically built up to analyze ambient aerodynamic field character and unburned coal particle distributions in that field. The inner diameter of the investigated rotary kiln was 3.5 m, and the length was 20 m. As shown in Fig. 1, primary air is blown from the four tunnels of burner, while secondary air is blown from outer space in rotary kiln.

Grid is integrated with few partitioned regions; denser mesh is placed locally where needs extra care. The calculated domain is divided into two regions, for the near hood region, structural tetrahedral mesh is used; as for the rest region; structural non-uniform hexahedral mesh is used.

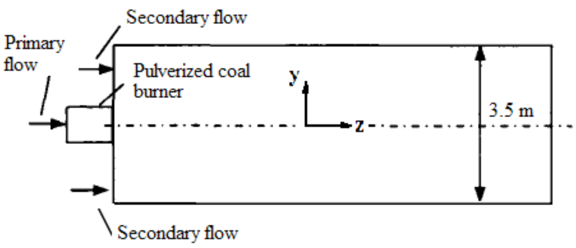

Fig. 1. Computational domain.

3.2. Numerical Method and Boundary Conditions

In the paper, particle-trajectory is taken to resolve two-phase flow, and *k-ε* turbulent model is used. Considering the field of gravity, trajectory of particle motion and particle distributions in the turbulent field which driven by four-channels swirling burner is intently focused to provide a theoretical basis on combustion research in the industrial rotary kiln.

Both primary and secondary airs are set as velocity -inlet and pressure-outlet. 5 sets of operating condition are indicated in Table 1, comparison with condition 1 by varying pulverized coal particle diameters, swirling angle, inner and external flow blowing speed, etc., respectively.

Table 1. Initial velocity of the air duct inlets under different working conditions.

Conditions	Primary airflow				V_{ecf}
	V_{zxf}	V_{mf}	V_{nf}	V_{wf}	
Units	m/s	m/s	m/s	m/s	m/s
1	116	25.25	71.575	310.18	13.085
2	116	25.25	60	310.18	13.085
3	116	25.25	85	310.18	13.085
4	116	25.25	71.575	260	13.085
5	116	25.25	71.575	360	13.085

4. Characteristics of Motion Trail and Distributions of Coal Particles

4.1. Two-phase Turbulence Features

Fig. 2 indicates that, from burner tunnel, swirling flow is spread into the space at a proper angle. During this process, the primary air decreases to 0 gradually, and then even reaches to negative (minimum at -22.2 m/s). Meanwhile, asymmetric heart-shape central backflow is formed and bringing more coal particles into central backflow field under the force of gravity. It extends residence time of particles in the backflow, which could promote particles mixed and enhance combustion efficiency.

Mass distributions on the longitudinal section and cross section are shown in Fig. 3. It can be found that, the barycenter of coal particles move slowly toward negative direction of y axis and, observed from cross section, the region occupied by coal particles gradually expends. This indicates that, particles diffuse gradually and settled down slowly.

Fig. 4 shows the distributions of coal particle when they are just spread into the kiln by annular tunnel. In this figuration, it is clearly observed that, the shape of particle distributions is like asymmetric 'pommel horse' at z = 0.5 m. The reason for asymmetric is that particles are blown in through 10 tunnels, then distributed in random trajectory. Therefore, central backflow region is shaped into an asymmetric domain from observation of transverse section. In addition, the region occupied by denser particles is surely with less air flow. That provides an explanation for the vector distribution character in the centre of kiln in Fig. 2 At z = 2 m, particle distributed shape, from unimodal, becomes to bimodal, because particle start to concentrate into beam under the motion of central backflow. And, at z = 6 m, particles are about to diffuse and mostly distributed under y axis due to gravity begins to play a dominant role.

Fig. 5 is observed in different axis. At z = 2~6 m, coal mass are mainly centralized on and around central axis (y=0) indicating coal particles are mainly distributed in the central region of kiln; while, the mass located at y = -0.1 m is larger than at y = 0.1 m, and at z = 7 m, coal mass is almost as the same as at y = 0. Because, particles settle down acted by gravity. At y = -2 m and y = -5 m, mass located is gradually reducing, meanwhile, at y = -5 m, particles begin to distribute locally after z = 3 m. This illustrates that, after spread into kiln, particles are blown straightly in the first 3 m, after that, they begin to diffuse into the space between y = ±5 m (cross section).

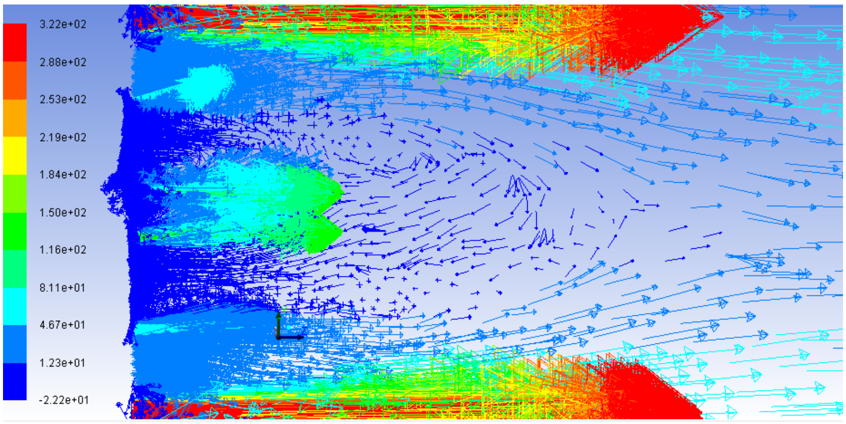

Fig. 2. Velocity vectors in the vertical section.

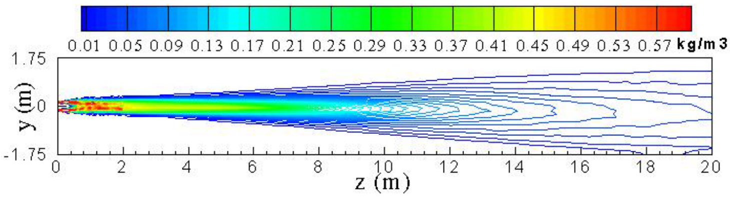

(a)

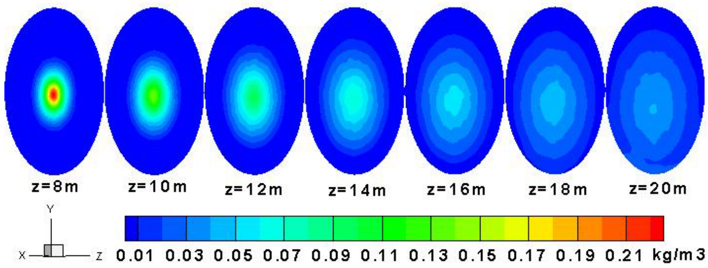

(b)

Fig. 3. Particle distributions in (a) longitudinal section and (b) cross section of kiln.

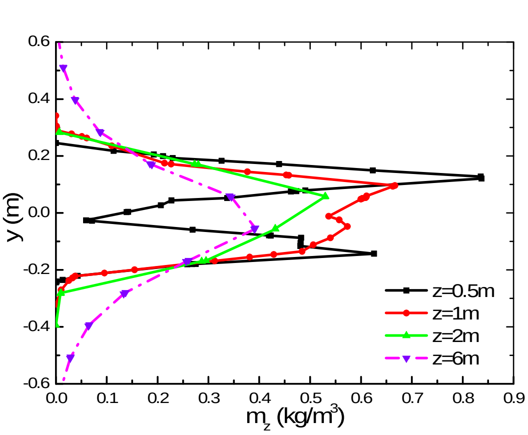

Fig. 4. Coal particle distributions near nozzle.

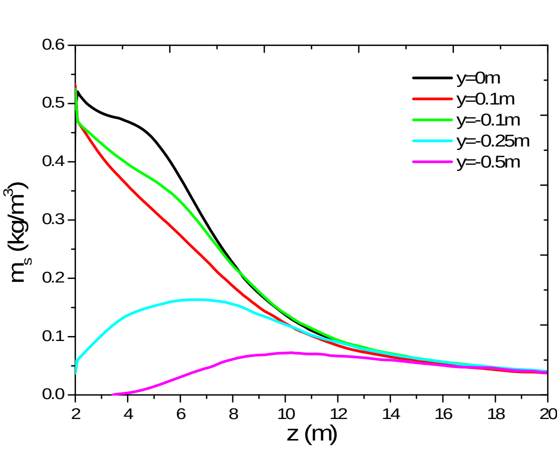

Fig. 5. Coal particle distributions in different axis

4.2. The Influence of Particle Size on Coal Distributions

A comparison is made to research the relationship between particle size and distributions on the operating condition 1, in which 3 sets particle of different diameters (60, 86.4, 120 μm) are chosen. Fig. 6 shows the mass distribution along the central axis of rotary kiln. This curve also indicates the extent of particle diffusion. It is obvious that, after blown from the flow inlet, particles gather at by the suction of central backflow at z = 2 m where reach to the highest mass. Then, diffusion occurs, at z = 12 m, diffusion retards, finally spread to the whole space.

In addition, from the comparison mentioned above, it is found that, in the range z = 2 m ~ 6 m, the smaller of particle size, the larger mass, hence, the slope of curve increases. It seems that smaller particles diffuse easily than larger ones. When turbulent intensity grows, diffusion aggravates too; with smaller size, particles more likely go by airflow.

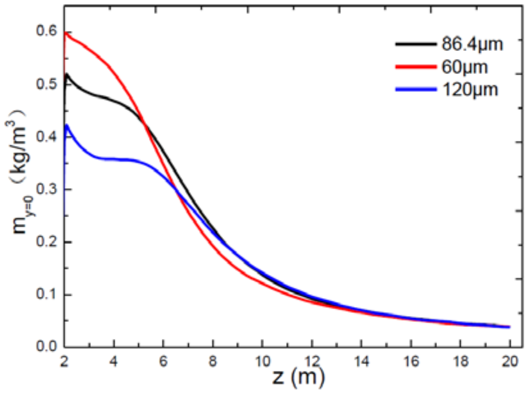

Fig. 6. Particle distributions along central axis.

4.3. The Influence of Internal Flow on Coal Distributions

The following is the research focused on the effect of internal flow velocity. A comparison has been done by employing three internal flow velocities which are 71.575 m/s, 60 m/s and 85 m/s respectively. Fig. 7 shows that the tangential velocity definitely increase with larger internal flow velocity. In Fig. 8, from the coal particle distribution curves in the three conditions, the comparison is obvious. It validates the strong effect on particle motion brought by internal flow velocity, in other word, it can be considered as larger tangential velocity acts obviously. Through the comparison, it is known that, smaller internal velocity leads to smaller tangential velocity, but larger coal particle mass and more concentrated particles. This helps to form long and slender shaped flame.

In above, internal flow velocity should be controlled in proper range. When it cooperates with central flow and external flow in the appropriate behavior, well shaped flame and high combustion intensity are easily obtained.

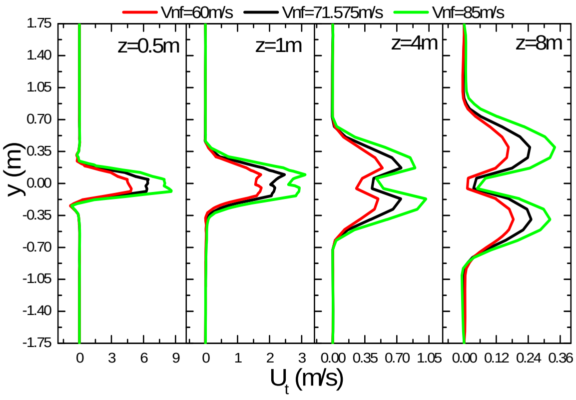

Fig. 7. Tangential velocity distributions along radial direction.

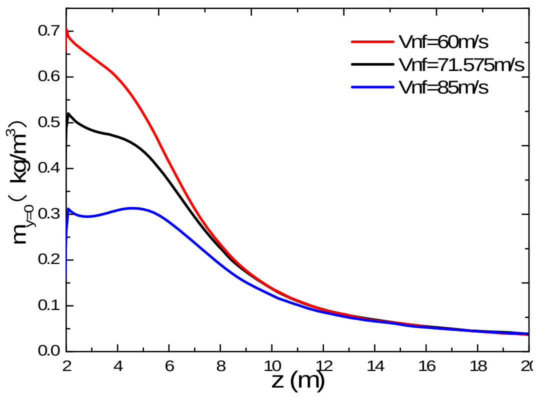

Fig. 8. Particle distributions along central axis.

4.4. The Influence of External Flow on Coal Distributions

High velocity external flow plays an important part in turbulent flow, which is adjacent to both secondary airflow and internal swirling flow, and critical to form central backflow and outer backflow. In Fig. 9, radial velocity is enhanced with the growth of external flow velocity. As external flow velocity is reaching 360 m/s, radial velocity tends to be more symmetrically distributed, leading to particles well-distributed and stable combustion.

With the alternating external flow, particle movements change accordingly. In Fig. 10, it validates the effect on particle motion brought by external flow velocity. Through the comparison, it is known that, larger external velocity leads to more stable distribution of radial velocity, coal particles tend to gathering rapidly. So, the coal has the largest mass at the 360 m/s external velocity. However, in the case, coal particles diffuse fast, till occupy full space of the rotary kiln.

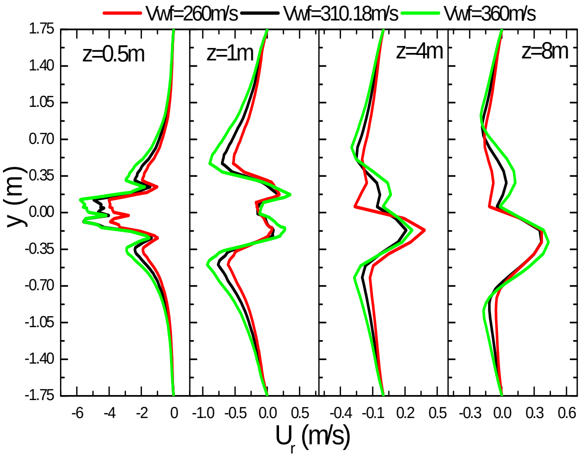

Fig. 9. Radial velocity distributions.

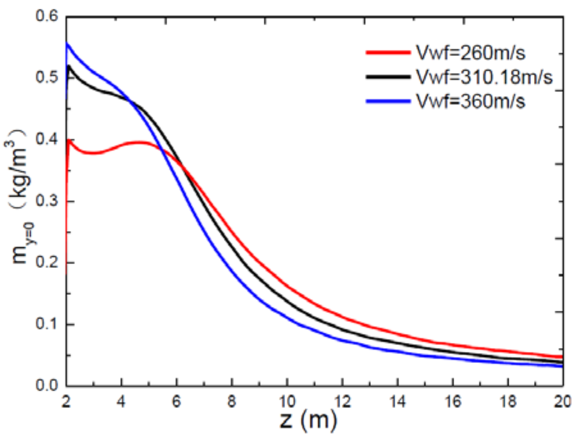

Fig. 10. Particle distributions along central axis.

In above, external flow velocity should be controlled in proper range. When it cooperates with central flow and internal flow in the appropriate behavior, well shaped flame and high combustion intensity are easily obtained.

5. Conclusion

The paper builds up a numerical model of cold solid-gas two-phase flow based on the kiln and four-channel burner. The results are shown below:

(1) The smaller pulverized coal particle size is, the less affected by gravity, the more affected by turbulence flow, more evenly distributed in kiln.

(2) With increasing velocity of internal flow, the degree of disturbance and diffusion raises, while tangential velocity boosts as internal flow velocity increases, which will be adverse to achieve long-slender shaped flame and converge particles.

(3) Improvement on external flow velocity leads to activate particles to converge into a bundle faster. However, out of central backflow region, particles are easily to blown away and diffusion aggravates.

Nomenclature

m_s	coal particle mass located at certain axis, kg/m^3
m_y	coal particle mass located on radial direction, kg/m^3
$m_{y=0}$	coal particle mass located at y=0 (central axis) , kg/m^3
U_r	radial velocity, m/s
U_s	longitudinal velocity, m/s
U_t	tangential velocity, m/s
V_{mf}	coal spread airflow velocity, m/s
V_{nf}	internal swirling flow velocity, m/s
V_{wf}	external flow velocity, m/s
V_{zxf}	central flow velocity, m/s
V_{ecf}	secondary airflow, m/s

References

[1]. Andrzej Smolarz, Andrzej Kotyra, Waldemar Wojcik, Javier Ballester, Advanced diagnostics of industrial pulverized coal burner using optical methods and artificial intelligence, *Experimental Thermal and Fluid Science*, Vol. 43, 2012, pp. 82-89.

[2]. E. Mastorakos, A. Massias, C. D. Tsakiroglou, D. A. Goussis, V. N. Burganos, A. C. Payatakes, CFD predictions for cement kilns including flame modeling, heat transfer and clinker chemistry, *Applied Mathematical Modeling*, Vol. 23, 1999, pp. 55-76.

[3]. Kaustubh S. Mujumdar, Vivek V. Ranade, CFD modeling of rotary cement kilns, *Asia-Pacific Journal of Chemical Engineering*, Vol. 3, 2008, pp. 106-118.

[4]. Jianping Jing, Zhengqi Li, Qunyi Zhu, Zhichao Chen, Lin Wang, Lizhe Chen, Influence of the outer secondary air vane angle on the gas/particle flow characteristics near the double swirl flow burner region, *Energy*, Vol. 36, 2011, pp. 258-267.

[5]. Cristian H. Birzer, Peter A. M. Kalt, Graham J. Nathan, The influences of particle mass loading on mean and instaneous particle distributions in processing jet flows, *International Journal of Multiphase Flow*, Vol. 41, 2012, pp. 13-22.

[6]. Hao Zhou, Guiyuan Mo, Jiapei Zhao, Kefa Cen, DEM-CFD simulation of the particle dispersion in a two-phase flow for a fuel-rich/lean burner, *Fuel*, Vol. 90, 2011, pp. 1584-1590.

[7]. M. S. Manju, S. Sacithri, Three dimensional CFD simulation of pheumatic coal injection in a direct reduction rotary kiln, *Fuel*, Vol. 102, 2012, pp. 54-64.

[8]. A. Bermudez, J. L. Ferrin, A. Linan, L. Saavedra, Numerical simulation of group combustion of pulverized coal. *Combustion and Flame*, Vol. 158, 2011, pp. 1852-1865.

[9]. Federico Cangialosi, Francesco Di Canio, Gianluca Intini, Michele Notarnicola, Lorenzo Liberti, Giulio Belz, Pompilio Caramuscio, Experimental and theoretical investigation on unburned coal char burnout in a pilot-scale rotary kiln, *Fuel*, Vol. 85, 2006, pp. 2294-2300.

[10]. G. J. Nathan, J. Mi, Z. T. Alwahabi, G. J. R. Newbold, D. S. Nobes, Impacts of a jet's exit flow pattern on mixing and combustion performance, *Progress in Energy and Combustion Science*, Vol. 32, 2006, pp. 496-538.

[11]. T. P. Bhad, S. Sarkar, A. Kaushik, S. V. Herwadkar, Kiln with multi-channel burner for optimization of

flame profile, in *Proceedings of the 7th International Conference on CFD in the Minerals and Process Industries*, CSIRO, Melbourne, Australia, 2009, pp. 9-11.

[12]. Zhou Jiemin, Zhu Zaixin, Ma Aichun, Numerical simulation research on coal combustion in rotary kiln with multi-air channel coal burner, in *Proceedings of the International Conference on Intelligent Systems Design and Engineering Application*, 2012, pp. 1070-1073.

[13]. Ma Aichun, Zhou Jiemin, Li Wang Xing, CFD prediction of cold airflow field for multi-air channel pulverized coal burner in rotary kiln, in *Proceedings of the 37th Intersociety Energy Conversion Engineering Conference*, 2002, pp. 418-421.
